Further, this figure would mean that $Ni^+{=}CHCH_3$ could be formed in the ethane system beginning about 1.4-1.8 eV, consistent with the high-energy reactivity observed in Figure 1b.

In the Cu^+-isobutane system, the apparent threshold for $CuC_2H_4^+$ is $\simeq$2.8 eV (65 kcal/mol) (Figure 4c), which suggests that $D°(Cu^+{-}CHCH_3) \approx 36$ kcal/mol. In the Cu^+-ethane system, the threshold for $CuC_2H_4^+$ is 3-4 eV (69-92 kcal/mol), which would mean that $D°(Cu^+{-}CHCH_3)$ is between 9 and 32 kcal/mol.

(56) Fisher, E. R.; Armentrout, P. B., work in progress. This value is somewhat lower than the generally accepted literature value of 86 ± 6 kcal/mol.[43]

Also, the observation of H_2 and D_2 loss in the $Cu^+ + CH_3CD_3$ system is consistent with formation of Cu^+-ethylidene. Since the $Cu^+(3d^{10})$ species cannot form a covalent double bond, it is possible that this is a dative interaction in which a singlet $CHCH_3$ donates its lone pair of electrons to the empty 4s orbital of Cu^+. This is consistent with the very weak bond energy derived.

Acknowledgment. We thank Nick Pugliano and R. H. Schultz for performing some of the Co^+ experiments. We would also like to thank C. W. Bauschlicher for communicating results prior to publication. This work was supported by National Science Foundation Grant No. CHE-8796289.

Copper Coordination in Nitrous Oxide Reductase from *Pseudomonas stutzeri*

Haiyong Jin,[†] Hans Thomann,*[,†,‡] Catherine L. Coyle,*[,†] and Walter G. Zumft[§]

Contribution from the Corporate Research Laboratory, Exxon Research and Engineering Company, Annandale, New Jersey 08801, and Lehrstuhl für Mikrobiologie, Universität Karlsruhe, Kaiserstrasse 12, D-7500 Karlsruhe 12, West Germany. *Received May 2, 1988*

Abstract: The structure of the copper sites in the multicopper enzyme nitrous oxide (N_2O) reductase from *Pseudomonas stutzeri* has been studied by electron paramagnetic resonance (EPR) and electron spin echo (ESE) spectroscopies. Correlations between the enzyme activity and paramagnetic susceptibility, the pH dependence of the EPR spectra, and exogenous ligand binding were investigated. Two types of copper sites are identified: antiferromagnetically coupled ($J > 200$ cm^{-1}) dimeric sites and unusual Cu(II) sites. The EPR susceptibility arises from these Cu(II) sites and from binuclear mixed-valence Cu(I)/Cu(II) half-met sites which may be derived from partially reduced dimers. On average, six of the eight copper ions per protein are in the form of the EPR-silent binuclear type 3 dimers. At $g = 2.03$ in the EPR spectrum, the Fourier transform of the stimulated echo envelope reveals a complex spectrum with narrow lines at 1.5, 1.9, 2.5, 2.9, and 3.4 MHz and broad lines centered at 0.8 and 3.8 MHz. This spectrum is not typical of either blue (type 1) or square-planar (type 2) sites in copper proteins. However, with the exception of the lines at 2.5 and 3.4 MHz, the spectrum for N_2O reductase is remarkably similar to that observed for the Cu_A site in cytochrome c oxidase. This is the first direct evidence that the Cu_A site exists in an enzyme other than cytochrome c oxidase. The ESE envelope spectrum can be simulated by using three sets of ^{14}N quadrupole coupling parameters. Two of these are characteristic of the distal nitrogen on imidazole ligands bound to Cu(II). By analogy to the ESE envelope spectra for the Cu_A site in cytochrome c oxidase, these two imidazole ligands are coordinated to the Cu_A site in N_2O reductase. The third ^{14}N, which is most likely coordinated to the half-met site, has a quadrupole coupling that is close to that observed by nuclear quadrupole resonance (NQR) spectroscopy for amide nitrogen and to that deduced from ESE measurements for the distal nitrogen of substituted imidazoles in copper-imidazole complexes. However, in both cases the quadrupole asymmetry is much smaller than that deduced from the present data. Water accessibility of the copper sites was investigated by ESE envelope spectroscopy. The deuteron modulation frequency observed for all forms of the enzyme dialyzed against D_2O at different pH values indicates that the EPR-active copper sites are accessible to water. A 10-fold increase in catalytic activity was observed after dialysis of the enzyme at pH 9.8. No concomitant change in the nitrogen ESE envelope spectrum was observed, but a significantly deeper deuteron modulation was observed for the enzyme dialyzed against D_2O. The envelope waveform is characteristic of a directly coordinated deuterated ligand, most likely a water or hydroxide. The increase in EPR line width and paramagnetic susceptibility, also observed at high pH, suggests that a new EPR-active copper site that has more exchangeable protons is generated at high pH. However, a pH-induced protein conformation change or base-catalyzed proton exchange allowing enhanced solvent accessibility to the copper sites cannot be ruled out.

Nitrous oxide (N_2O) is reduced to dinitrogen by denitrifying bacteria as part of the anaerobic respiration of nitrate to dinitrogen. Nitrous oxide reductase is the enzyme that catalyzes the reduction of N_2O to N_2 and H_2O. The multicopper enzyme from *Pseudomonas stutzeri* (formerly *Pseudomonas perfectomarina*) has been isolated and purified to homogeneity. The enzyme contains about eight copper atoms per molecular weight 140 000 and is composed of two identical subunits.[1] No other metal ions have been detected by plasma emission studies. Several different forms of the enzyme have been prepared. The more active purple form is obtained by purifying the enzyme under anaerobic conditions.[2] Aerobic purification of N_2O reductase produces a pink form that contains less copper and is 2-5-fold less active. Preparative isoelectric focusing of the purple form results in the resolution of two protein bands with slightly different isoelectric points (an anodic band at pI = 4.97 and a cathodic band at pI = 5.06). A blue inactive form is obtained by reduction with excess dithionite or ascorbate. A high-pH form of the enyzme, prepared by dialysis against buffer at pH 9.8, has an activity approximately 10-fold higher than that of the same enzyme at pH 7.5.[3]

Most copper centers in proteins have been classified into three types: "blue" (type 1), "normal" (type 2), and dimeric (type 3),

[†] Exxon Research and Engineering Company.
* Authors to whom correspondence should be addressed.
[‡] Also at Department of Chemistry, State University of New York, Stony Brook, Stony Brook, NY 11794.
[§] Universität Karlsruhe.

(1) Zumft, W. G.; Matsubara, T. *FEBS Lett.* **1982**, *148*, 107-112.
(2) Zumft, W. G.; Coyle, C. L.; Frunzke, K. *FEBS Lett.* **1985**, *183*, 240-244.
(3) Coyle, C. L.; Zumft, W. G.; Kroneck, P. M. H.; Korner, H.; Jakob, W. *Eur. J. Biochem.* **1985**, *153*, 459-467.

0002-7863/89/1511-4262$01.50/0 © 1989 American Chemical Society

Table I. Various Forms of Nitrous Oxide Reductase

form	observations or characteristics
A (purple)	high-activity form; ca. 8 Cu per M_r 140 Da; isolated anaerobically (except IEF); 7-line EPR hyperfine splitting[2,3]
B (cathodic)	part of form A that focuses in IEF toward the cathode at pI = 5.06; integrity closest to native enzyme[3]
C (anodic)	part of form A that focuses in IEF toward the anode at pI = 4.97; integrity closest to native enzyme[3]
D (pink)	low-activity form; ca. 7 Cu per M_r; isolated aerobically; 4–5-lin EPR hyperfine splitting[1]
E (blue)	catalytically inactive; obtained from A, B, C, or D upon addition of reductant; largely featureless EPR; indications for presence of type I Cu[1-3]
F (pH 9.8)	form A after 24-h dialysis against 50 mM CHES buffer aT pH = 9.8. Specific activity increases 10-fold[3]

which are distinguished by their characteristic EPR and UV–visible spectroscopic properties.[4] Previous EPR and UV–visible data on N_2O reductase could not be readily described in terms of these three categories, indicating that N_2O reductase may have a novel copper center.[3] In this article, we report a further investigation of the copper sites by detailed EPR and ESE studies on the different forms of the enzyme as a function of temperature and pH. The copper sites were also probed by exogenous ligand-binding studies.

Experimental Section

N_2O reductase from *Pseudomonas stutzeri* (formerly *Pseudomonas perfectomarina*, ATCC 14405) was purified as previously described.[1-3] All manipulations were performed at 4 °C, and 25 mM Tris–HCl, pH 7.5, was used throughout unless otherwise stated. The different forms of the enzyme used in this study are described in Table I. N_2O reductase activity was monitored spectrophotometrically as reported previously.[2,3] Copper was detected by using inductively coupled plasma/atomic absorption spectroscopy. The protein concentration was determined by the method of Lowry et al.[5]

The EPR spectra were recorded on an X-band Varian E109 spectrometer equipped with an Oxford Instruments E9 helium flow-through cryostat and interfaced to a Digital Equipment Corp. (DEC) MINC-11 microcomputer. The spectra were digitized at 2048 points over the full sweep width by using a 12-bit analog-to-digital convertor and integrated directly on the MINC-11. The spin susceptibility was determined by using a $MoS_2(S_2CNEt_2)_3$ standard whose susceptibility was independently calibrated by using both a dc vibrating magnetometer and an NBS ruby standard. Parameters for recording EPR spectra were typically 100 G/min sweep rate, 10-G_{pp} modulation amplitude, 100-kHz modulation frequency, and 0.1-mW incident microwave power, depending on the temperature.

ESE data were recorded on a home-built spectrometer operating at 9.1 GHz.[6] All pulse timing intervals were derived from a home-built pulse programmer interfaced to a DEC LSI-11/73 minicomputer. Above 4.2 K, either an overcoupled TE_{102} microwave cavity or a slotted tube resonator mounted directly on the quartz insert Dewar of an Oxford Instruments E9 helium flow cryostat was used.[7] Below 4.2 K, a slotted tube resonator mounted in a Janis variable-temperature cryostat was used.[8] Typically, 400 data points were recorded in the time domain with 20- or 30-ns increments between data points and at a 100-Hz repetition rate. Fourier transformation was performed after subtracting the spin relaxation decay function by using a polynomial fit and zero filling to 2048 data points.

Experimental Results

EPR Studies. EPR spectra were recorded for the oxidized and reduced pink, purple, and cathodic forms of the enzyme as well as the purple enzyme at pH 9.8, over the temperature range 5–50 K. Representative spectra, recorded at 10 K, for the oxidized (active) and reduced (inactive) forms of the enzyme are shown in Figures 1 and 2, respectively. Spectra were recorded under a variety of operating conditions to check for possible line-shape distortion effects, particularly microwave power saturation and rapid passage effects. The onset of power saturation was established by determining the microwave power at which the signal intensity no longer doubled for a 6-dB change in incident power. At a given temperature, the onset of power saturation varied slightly (~20%) among the different forms of the enzyme. A more significant difference between saturation powers was observed between each of the oxidized and their respective reduced forms. In this case, power differences of a factor of 2 were typically observed at $T \sim 10$ K.

In previous EPR studies of this enyzme, four- to seven-line copper hyperfine patterns with 35–40-G hyperfine splittings were

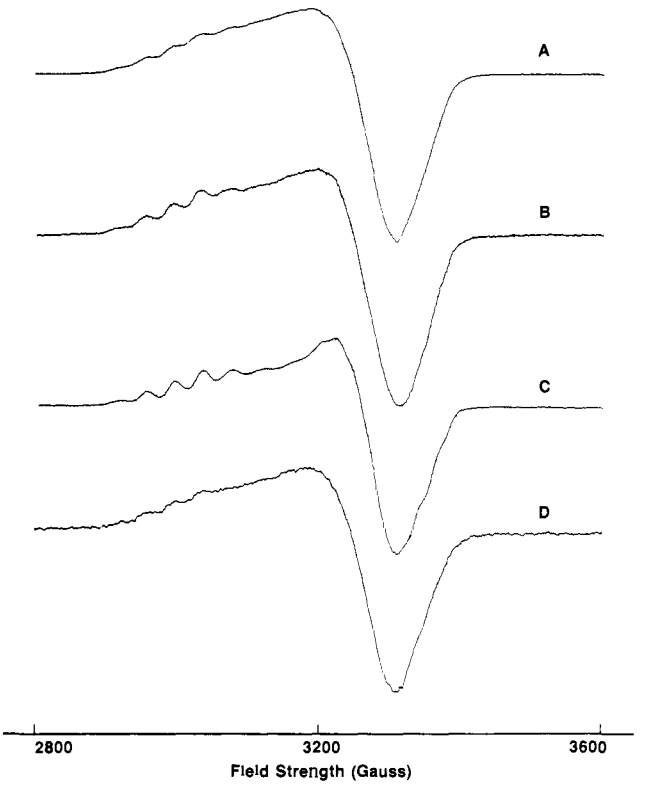

Figure 1. X-band EPR spectra taken at 10 K for various oxidized forms of N_2O reductase: (A) pink form; (B) purple form; (C) cathodic form; (D) purple form at pH 9.8.

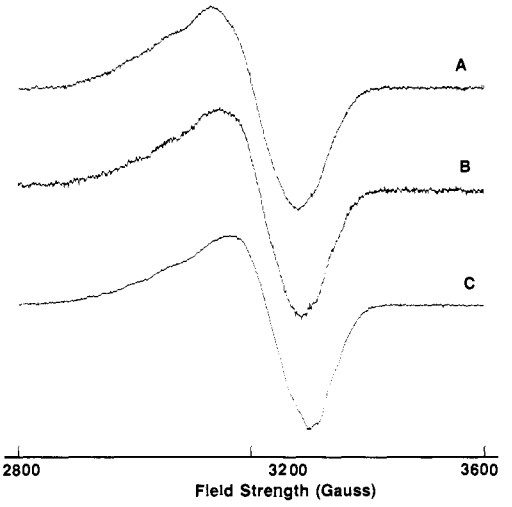

Figure 2. X-band EPR spectra taken at 10 K for various reduced forms of N_2O reductase: (A) pink; (B) purple; (C) cathodic.

(4) Malkin, R.; Malmström, B. G. *Adv. Enzymol. Relat. Areas Mol. Biol.* **1970**, *33*, 177–244.
(5) Lowry, O. H.; Rosebrough, N. J.; Farr, A. L.; Randall, R. J. *J. Biol. Chem.* **1951**, *193*, 265–275.
(6) (a) Thomann, H.; Tindall, P. J.; Bernardo, M. *Anal. Instrum.*, in press. (b) Thomann, H.; Dalton, L. R.; Pancake, C. *Rev. Sci. Instrum.* **1984**, *55*, 389–398.
(7) Lin, C. P.; Bowman, M. K.; Norris, J. R. *J. Magn. Reson.* **1985**, *65*, 369–374.
(8) Mehring, M.; Freysoldt, F. *J. Phys.* **1980**, *13*, 894–896.

observed in the $g_{\parallel}$ region of the X-band spectrum.[3,9] As shown in Figure 1, these unusually small hyperfine splittings were also observed for the present samples, and the number of hyperfine lines observed (at a given temperature) depended on the form of the enzyme. At 10 K (Figure 1) a direct correlation between enzyme activity and resolution of copper hyperfine splitting was observed. An exception to this trend was the pH 9.8 form (Figure 1D), which had the highest activity but the poorest resolution of the hyperfine splitting pattern. At 10 K, the EPR line width decreased in the order pink, purple, and cathodic, with the purple sample at pH 9.8 again exhibiting an anomalously broad line, comparable to the line width for the pink form. The resolution of the hyperfine splitting also depended on the temperature, and the optimum temperature varied for each form of the enzyme.

The broadening of the line width and the poorer resolution of the hyperfine splittings may indicate that subtle differences exist in the copper coordination among the different forms of the enzyme. Alternatively, it may indicate that there are different EPR-active copper sites, and the relative concentration of these sites depends on the form of the enzyme. In this case, copper sites with slightly different g values but similar hyperfine splittings may be present in different amounts for the different forms of the enzyme. This is consistent with the observation that the hyperfine splittings for each of the two individual components (cathodic and anodic) of the purple form are better resolved than that observed for the purple form itself. The resolution is better for the cathodic form than for the anodic form, consistent with the higher enzyme activity of the cathodic form. In addition, the apparent $g_{\parallel}$ value for the cathodic form is shifted slightly with respect to the anodic form. This can account for the lower resolution observed for the purple form, which is actually a mixture of the cathodic and anodic forms. It is likely that at pH 9.8, some of the sites that were EPR silent at pH 7.5 become EPR active. If these new sites have slightly different EPR properties than those present at pH 7.5, the superposition of the EPR signals would result in an increase in the EPR susceptibility, broader EPR line width, and decreased resolution of the hyperfine splittings.

An unusual feature of N_2O reductase is that an EPR signal is still observed after the enzyme is reduced with an excess of dithionite. Although it is possible that N_2O reductase has some copper sites with an anomalously low reduction potential, a more reasonable explanation is that the EPR is due to the inaccessibility of some of the copper sites to the reductant. The spectra for each of the reduced enzymes are shown in Figure 2. Weak hyperfine splittings characteristic of type 1 (blue) copper are observed for the reduced enzymes. Additional hyperfine structure is observed for the reduced purple enzyme at pH 9.8; however, this enzyme became partially denatured upon addition of excess dithionite as evident by the formation of a precipitate. Recent resonance Raman results on the reduced enzyme also suggested that the copper sites are typical type 1, blue copper sites.[10]

The temperature dependence of the EPR susceptibility for the pink, purple, and cathodic forms of the enzyme are shown in Figure 3. The inverse of the molar susceptibilities of the oxidized enzyme are shown in Figure 3A, and the inverse of the "normalized" susceptibilities, where $\chi_{norm} = \chi_{ox} - \chi_{red}$, are plotted in Figure 3B. EPR susceptibilities for all forms of the enzyme (χ_{ox}, χ_{red}, and χ_{norm}) follow the Curie law $1/\chi = A(T - T_c)$ with $T_c < 2$ K (the experimental precision on the Curie temperature). The percentage of the copper that is EPR active can be calculated from the slope of the inverse susceptibility curves in Figure 3. These results are summarized in Table II. Both χ_{ox} values (Figure 3A) and χ_{norm} (Figure 3B) decrease monotonically with enzyme activity for the pink, purple, and cathodic enzymes. Differences in EPR susceptibility observed between the enzyme from different preparations correlate with corresponding differences in enzyme activity. A notable exception is observed for purple enzyme at pH 9.8, which had the highest activity and the highest susceptibility. This is consistent with the formation of new EPR-active sites at high pH.

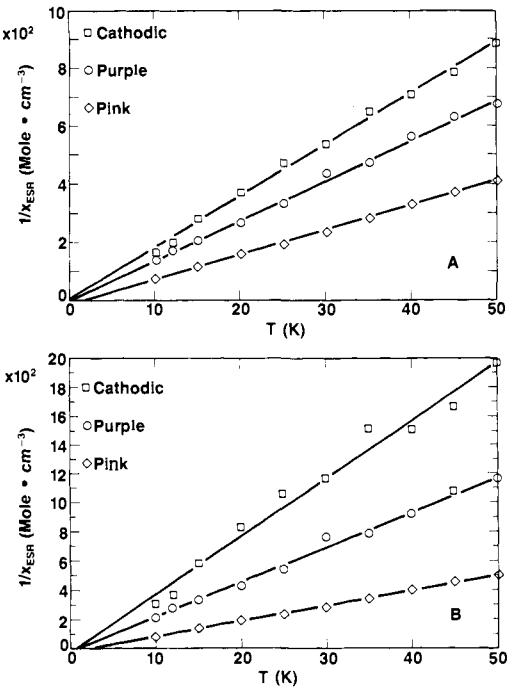

Figure 3. Temperature dependence of inverse EPR susceptibility for various forms of N_2O reductase: (A) total susceptibility for the oxidized enzymes; (B) normalized susceptibility obtained by subtracting the susceptibility for the reduced enzymes from (A).

Table II. List of Percentage of Cu That Is EPR Active, from the EPR Susceptibility Measurements on N_2O Reductase[a]

form of enzyme	oxidized	"normalized"
pink	31	26
purple	19	11
cathodic	15	7
pH = 9.8 (from purple)	29	

[a] Measurement made within temperature range of 10–50 K. Curie–Weiss formula was used with Curie temperature of all forms less than 2.0 K, which is the experimental precision on Curie temperature.

Between 15 and 30% of the copper sites are EPR active depending on the form of the enzyme, the pH, and the particular enzyme preparation. The magnetic coupling between these EPR-active sites is very small, as indicated by the very small values of T_c. No EPR signal was observed near $g = 4$ as would be expected for weakly coupled copper dimers. The remaining copper is EPR inactive and most likely associated with strongly coupled Cu(II) dimers with an antiferromagnetic exchange coupling greater than 200 cm^{-1}. The EPR-silent sites are not likely to be Cu(I) sites because the EPR is not affected by ferricyanide oxidation.

The enzyme activity decreases and the number of copper sites that are EPR active increases upon lowering the pH from 7.5 to 6.0. Furthermore, the seven-line hyperfine pattern sharpens significantly on lowering the pH from 7.5 to 6.0 (compare Figures 4A (purple, pH 7.5) and 5A (purple, pH 6.0)). These results are similar to the trends observed for hemocyanin and tyrosinase where the concentration of the mixed valence Cu(I)/Cu(II) half-met sites increases upon lowering the pH.[11] These observations motivated exogenous azide-binding studies as a spectroscopic probe of the copper sites. The addition of azide inhibits N_2O reductase activity and reduces the EPR susceptibility. The relative change in susceptibility is sensitive to the pH and to the amount of azide used. At pH 6.0, a 25% decrease in the number of copper sites

(9) Snyder, S. W.; Hollocher, T. C. *J. Biol. Chem.* **1987**, *262*, 6515–6525.
(10) Dooley, D. M.; Moog, R. S.; Zumft, W. G. *J. Am. Chem. Soc.* **1987**, *109*, 6730–6735.
(11) Solomon, E. I.; Penfield, K. W.; Wilcox, D. E. *Struct. Bonding* **1983**, *53*, 1–57, and references therein.

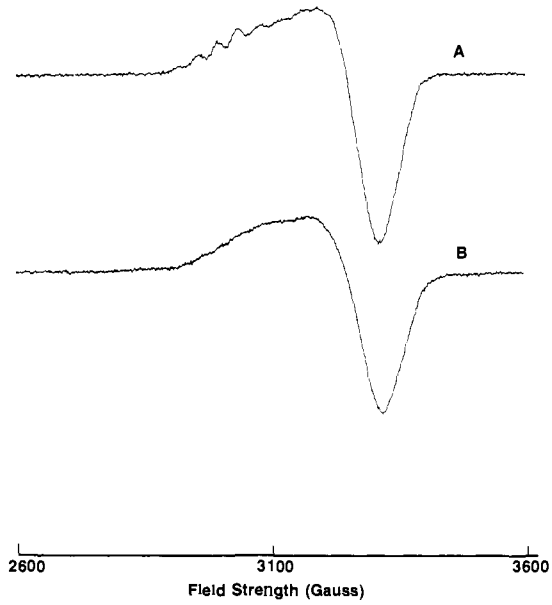

Figure 4. X-band EPR spectra (A) for oxidized purple enzyme at pH 7.5 and (B) after the addition of a 400-fold excess of azide over copper.

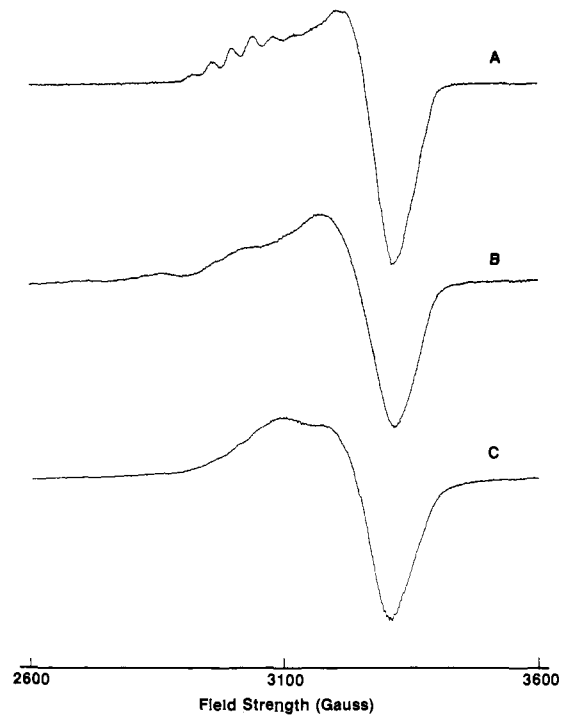

Figure 5. X-band EPR spectra (A) for oxidized purple enzyme at pH 6.0, (B) after adding a 300-fold excess of azide over copper, and (C) following dialysis for 4 h after the azide addition.

observed by EPR is obtained with a 2500-fold excess of azide. At pH 7.5, a 25% decrease was also observed by using only a 400-fold excess of azide. Addition of azide also resulted in the complete loss of the seven-line hyperfine structure in the EPR spectrum (Figure 4B). In addition, new weak hyperfine splittings characteristic of square-planar, type 2 copper, were observed (Figure 5B) for the sample at pH 6.0. Dialysis to remove excess azide and any type 2 Cu not bound to the protein did not restore the original EPR spectrum (Figure 5C) and resulted in the loss of the type 2 Cu and a 20% decrease in EPR susceptibility compared to the original value. The resulting EPR spectrum (Figure 5C) recorded at 10 K suggests a more isotropic magnetic interaction, consistent with rapid electron exchange between the two copper atoms of a half-met site.[11] These results suggest that azide binds irreversibly to the EPR-active sites.

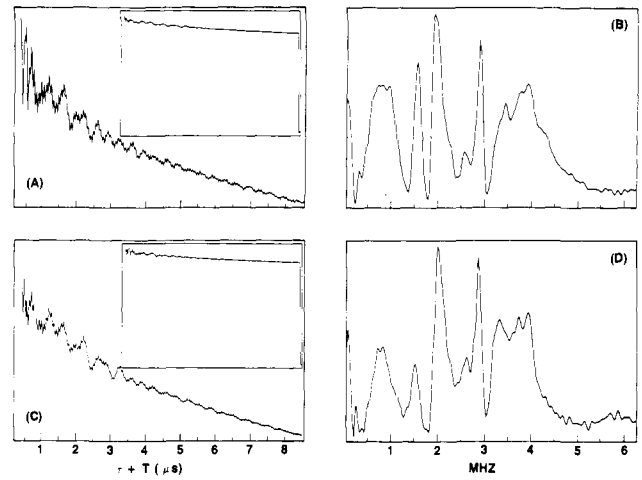

Figure 6. Time domain electron spin-echo envelope wave forms for oxidized and reduced N_2O reductase recorded at T = 1.8 K: (A) oxidized pink (aerobically isolated); (C) oxidized cathodic (anaerobically isolated); (B) and (D) are the Fourier transforms of (A) and (C), respectively. Other conditions: τ = 0.14 μs, B_0 = 3280 G; g = 2.03. Inserts of the time domain wave forms show the base line at the end of the data collection period.

Mechanisms by which azide binding can reduce the number of paramagnetically active sites are by oxidation of the cuprous ion in a half-met site, by bridging two uncoupled cupric ions to form a diamagnetic dimer, or by bridging a half-met (or dimer) site with a cupric ion to form a trimer. In hemocyanin and tryosinase, azide bridges the binuclear coupled copper site and reduces the strong antiferromagnetic exchange coupling between the coppers.[11] For this type of binding, azide addition would be expected to increase, not decrease, the EPR susceptibility. On the other hand, azide also binds to the binuclear copper site in laccase, but not as a bridging ligand.[11] In this case, the EPR susceptibility would not be expected to change with addition of azide. Neither of these two binding mechanisms appear to be operative in N_2O reductase since the EPR susceptibility decreases after azide addition. Two binding mechanisms consistent with the decrease in EPR susceptibility are for azide to bridge two closely lying Cu(II) ions or for the azide to bridge a cupric ion with a half-met site, forming effectively a copper trinuclear site. In either case, the azide bridging can increase the dipolar and exchange coupling between the EPR-active copper ions to render them EPR silent. The Cu sites that remain EPR active after azide addition can be attributed to half-met sites where azide is bound, but not as a bridging ligand, or to the azide bridging of Cu(II) ions with EPR-silent dimers, forming a trinuclear site. The nonbridged binding of azide can modify the copper hyperfine splittings (observed in the EPR spectrum) without modifying the EPR susceptibility.

ESE Studies of Nitrogen Coordination. The ESE envelope time domain wave forms observed at T = 1.8 K for the oxidized pink and cathodic enzyme at pH 7.5 are shown in Figure 6A,C. The most striking feature of the data is the extremely shallow modulation depth, roughly only 5% of the total signal intensity. The shallowness of the modulation depth is clearly evident by noting the modulation depth compared to the true base line at longer time values, shown as inserts in Figure 6. The shallow modulation depth observed on the wave forms for N_2O reductase is in sharp contrast to that observed for most other copper proteins where intense modulation, typically 25% or more of the echo intensity, is observed for data recorded under similar experimental conditions.[12]

(12) (a) Mims, W. B.; Peisach, J. In *Biological Magnetic Resonance*; Berliner, L. J., Reuben, J., Eds.; Plenum Press: New York, 1981; Vol. 3, pp 213–263. (b) Mims, W. B.; Peisach, J. In *Biological Applications of Magnetic Resonance*; Shulman, R. G., Ed.; Academic Press: New York, 1979; pp 221–269.

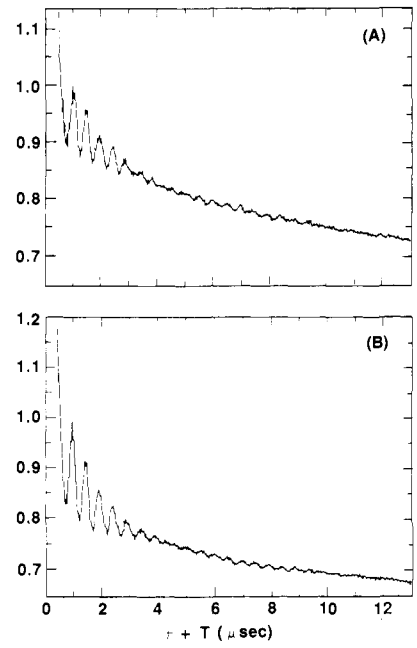

Figure 7. Time domain spin echo envelope data for oxidized (A) purple enzyme at pH 7.5 and (B) purple enzyme at pH 9.8, enzyme dialyzed against D_2O buffer. The intensities were normalized against the first peak in the modulation for easy comparison of the relative modulation depths. Spectra were recorded at T = 5 K, τ = 0.24 μs; other conditions are the same as for Figure 4.

Low-frequency oscillations are observed on the wave forms for the oxidized but not on those for the reduced enzyme. The identification of these modulation frequencies is facilitated by Fourier transformation to obtain the ESE envelope spectra, shown in Figure 6B,D, for the oxidized pink and cathodic enzymes. In addition to the proton peak at 13.6 MHz (not shown), complex spectra comprised of narrow lines at 1.5, 1.9, 2.5, 2.9, and 3.4 MHz and broad lines between 0.7–0.9 and 3.6–4.0 MHz are observed for the oxidized pink and cathodic enzyme. The modulation frequencies are typical for nuclear quadrupole transitions observed for nitrogen atoms coordinated to Cu(II).[12,13] When the echo envelope modulation depth is extremely shallow, as in the present case, the assignment of peaks below 0.5 MHz becomes unreliable because low-frequency peaks can be introduced by subtraction of the echo decay function. Although the paramagnetic susceptibility depends on the form of the enzyme, very little difference is observed in the low-temperature echo envelope spectra, as evident in Figure 6B,D.

ESE Studies of the Base-Activated Enzyme. A 10-fold increase in catalytic activity has been observed after dialysis of the enzyme in buffer at pH 9.8.[3] As noted above, a 50% increase in EPR susceptibility was observed for the enzyme at pH 9.8, but no significant change was observed in the ESE modulation spectrum. Differences were observed in the deuteron modulation pattern for all forms of the enzyme dialyzed against D_2O. The wave forms for the purple oxidized enzyme at pH 7.5 and at pH 9.8 are shown in Figure 7A,B, respectively. To facilitate comparison of the modulation depths, the echo amplitudes in Figure 7A,B have been normalized to the same vertical scale. It is apparent that the deuteron modulation depth for the enzyme at pH 9.8 is substantially deeper than that observed for the same enzyme at pH 7.5. The modulation depth of the purple enzyme at pH 9.8 is also substantially deeper than observed for the cathodic form at pH 7.5 (not shown).

A more direct demonstration of the deeper deuteron modulation on the purple enzyme at pH 9.8 is obtained by dividing the time domain wave form for the pH 9.8 sample by the time domain wave form for the purple sample that was used to prepare it, as shown in Figure 8A. When more than one nucleus is coupled to the

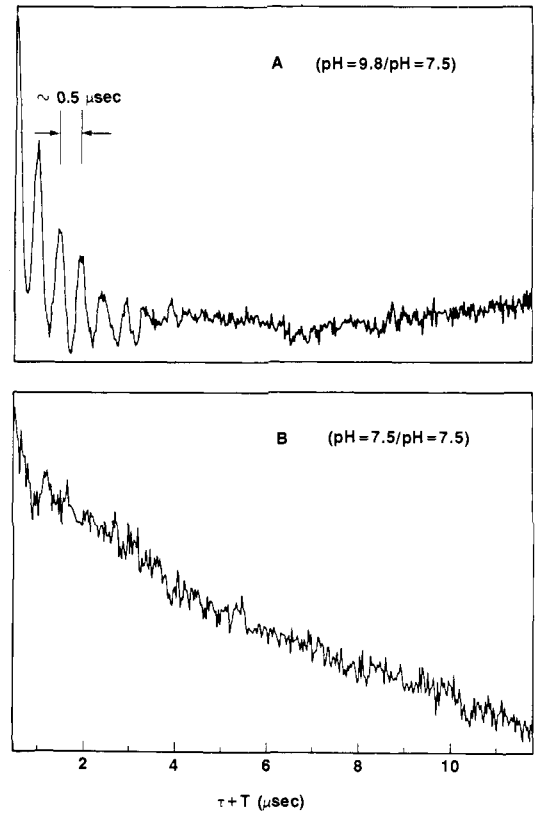

Figure 8. Ratio of spin-echo envelope time domain wave forms for various oxidized enzymes dialyzed against Tris buffer in D_2O: (A) purple at pH 9.8 over purple at pH 7.5; (B) Purple at pH 7.5 over cathodic at pH 7.5.

paramagnetic center, the total modulation depth depends on the product of the modulation depth due to each nucleus per copper center. For data collected under identical experimental conditions, the ratio of two time domain wave forms isolates any differences in modulation depth between the waveforms. The deuteron modulation period is clearly visible in the ratio of time domain wave forms as shown in Figure 8A. The ratio analysis was also performed by dividing the time domain wave forms of the purple by cathodic samples, both at pH 7.5, as shown in Figure 8B. In this case, only a smooth decay and no deuteron modulation is observed in the ratio of the two wave forms.

The deuteron modulation may arise from water or hydroxide in the inner or outer copper coordination sphere or from labile protons associated with the copper site. On the basis of comparison to the deuteron modulation data observed for amine oxidase[14] and several other Cu(II) complexes,[15] the modulation pattern observed is consistent with the presence of a directly coordinated deuterated ligand.

The deeper deuteron modulation associated with the oxidized purple enzyme at pH 9.8 indicates that there are more deuterons associated with the EPR-active sites at high pH. The increased susceptibility observed at pH 9.8 suggests that these additional deuterons result from a new EPR-active site generated at higher pH that has more deuterons associated with it than the EPR-active sites present at pH 7.5. Dissociation of the EPR-silent dimeric copper sites at high pH has previously been invoked by Solomon and co-workers to account for similar changes in the EPR spectra of binuclear copper sites.[11]

An alternate interpretation is that the deeper modulation at high pH arises from additional water or hydroxide in the inner

(13) Mims, W. B.; Peisach, J. *J. Chem. Phys.* **1978**, *69*, 4921–4930.

(14) McCracken, J.; Peisach, J.; Dooley, D. M. *J. Am. Chem. Soc.* **1987**, *109*, 4064–4072.

(15) (a) Mims, W. B.; Peisach, J.; Davis, J. L. *J. Chem. Phys.* **1977**, *66*, 5536–5550. (b) Suryanarayana, D.; Narayana, P. A.; Kevan, L. *Inorg. Chem.* **1983**, *22*, 474–478. (c) Anderson, M. W.; Kevan, L. *J. Phys. Chem.* **1986**, *90*, 6452–6459.

or outer coordination sphere of the copper that is EPR active at pH 7.5. This increased proton accessibility would be consistent with either a pH-induced protein conformational change or base-catalyzed proton exchange allowing enhanced access to the copper sites.

Discussion

According to the EPR susceptibility data, an apparent inverse correlation exists between the activity of the enzyme and the number of copper sites observed by EPR. Nevertheless, EPR and ESE studies provide important information about the catalytically active copper sites. EPR and ESE experiments are used to systematically follow changes in the structure of the EPR-active sites between the different enzyme forms. Furthermore, the number of EPR-active sites can be reversibly increased by changing the pH, in effect "turning on" the EPR-silent copper sites for spectroscopic study. Additionally, exogenous ligands can be used as spectroscopic probes of EPR-silent sites. Such experiments have been of considerable value in elucidating the structure of the EPR-silent sites in other binuclear copper enzymes such as hemocyanin and tyrosinase.[11] Finally, the results of the EPR and ESE experiments are correlated with other experiments including UV–visible absorption,[3] extended X-ray absorption fine structure (EXAFS),[16] resonance Raman,[10] and chemical analysis[1-3] to develop a consistent spectroscopic model of the catalytically active copper sites.

The hyperfine pattern in the EPR spectrum of N_2O reductase is not characteristic of either type 1 or type 2 centers in copper proteins.[17] One possibility is that the spectrum arises from the overlap of two type 1 copper spectra with $A_\parallel \sim 80$ G and a relative shift in $g_\parallel \sim A_\parallel/2$. This would result in an eight-line hyperfine pattern (the eighth line is not resolved) with equal line intensities, in rather poor agreement with the approximately 1:2:3:4:3:2:1 intensity ratio observed in the experimental spectra. Two other possibilities are that the unusual hyperfine pattern arises from the superposition of spectra from two type 1 copper sites with unusually small copper hyperfine couplings or from a mixed-valence Cu(I)/Cu(II) half-met site. A seven-line copper hyperfine pattern with an intensity ratio of 1:1:1:2:1:1:1 can be obtained for two type 1 coppers if the $A_\parallel$ hyperfine coupling is $\sim$38.5 G (which is unusually small) and if the shift in $g_\parallel$ between the two sites is also approximately equal to $A_\parallel$ so that only one line of the two four-line hyperfine patterns overlaps. On the other hand, a seven-line hyperfine pattern with an intensity ratio 1:2:3:4:3:2:1 and a hyperfine splitting one-half the value of the usual blue copper value is expected for a mixed-valence half-met site in which the unpaired electron spin density is shared equally between the two copper ions. The binuclear half-met site provides a natural mechanism for more extensive delocalization of the paramagnetic electron, compared to the usual blue copper center. This delocalization provides a mechanism for reducing the unpaired electron spin density on a particular ligand, consistent with the shallow modulation depth and unusually small contact hyperfine coupling observed in the ESE experiments. While it would be highly fortuitous to obtain the relationship between the two unusual type 1 coppers, where $A_\parallel$ is exactly one-half the value typically observed for type 1 copper, it is not possible, based on the EPR results alone, to unambiguously distinguish between a mixed-valence half-met site and these unusual type 1 sites. However, EPR experiments at other microwave frequencies[17] and the ESE results discussed below indicate that the EPR spectrum is comprised of contributions from both the half-met and the unusual Cu(II) type 1 sites.

The electron spin echo modulation data for N_2O reductase differs markedly from that observed for most other copper proteins.[12] Intense (typically 25% or more of the echo intensity) low-frequency modulation on the echo envelope wave forms is generally observed for all copper proteins containing type 1 or type 2 Cu(II) centers. This arises from the interaction of the paramagnetic electron on the Cu(II) ion with a nitrogenous ligand, usually the distal (N_1) nitrogen on a coordinated imidazole ligand. Nuclear quadrupole transitions on this nitrogen can give rise to up to three peaks for each of the electron spin manifolds. The actual number of peaks observed depends on the relative magnitudes of the quadrupole and hyperfine couplings and on the hyperfine anisotropy and quadrupole asymmetry.[12] When the applied magnetic field is chosen so that the nuclear Larmor frequency will be canceled by the hyperfine coupling in one of the electron manifolds, three narrow pure nuclear quadrupole transitions are observed below 1.7 MHz in the echo envelope spectrum. In addition, a broader line near 4.0–4.5 MHz, corresponding to the "double-quantum" nuclear transition in the other electron manifold, is usually observed. In contrast, an extremely shallow modulation depth (approximately 5% of the echo intensity) and uncharacteristic peaks in the modulation spectrum are observed for N_2O reductase. The spectra for N_2O reductase also contain many more peaks than are usually observed for type 1 or type 2 Cu(II) proteins. It is not likely that these additional peaks are due to combination frequencies arising from the coupling to more than one magnetically equivalent nitrogen (from more than one magnetically equivalent imidazole ligand on the same Cu(II) complex)[18] because the coefficients of the product frequencies will be extremely small due to the extremely shallow modulation depth.

One possible interpretation of these results is that the paramagnetic center in N_2O reductase is not a paramagnetic Cu(II) site. However, the EPR spectrum clearly exhibits resolved Cu nuclear hyperfine splittings (albeit with an unusual hyperfine coupling pattern) that are not observed in the spectrum of the reduced inactive enzyme. The low-frequency components in the echo envelope modulation pattern are also not observed for the reduced enzyme. Furthermore, only Cu is found by chemical analysis, the enzyme is inactivated, and no EPR signal is observed after Cu is removed from the enzyme.

Another possibility is that the echo envelope spectrum does not arise from an endogenous ligand but rather from the interaction with nitrogen atoms in the Tris buffer. Interaction with nitrogen from the Tris buffer was checked by repeating the ESE experiments on protein that was dialyzed against phosphate buffer. The spectra for these samples gave spectra identical with the samples run in Tris buffer, ruling out the possibility that the low-frequency modulation on the echo envelope wave form arises from interaction with a nitrogen in the buffer.

Numerical simulations were used to aid in identifying the possible nitrogen-containing ligands giving rise to the modulation spectrum observed for N_2O reductase. Following the work of Mims,[19] spectra were simulated by using the truncated Hamiltonian:

$$\hbar H_\pm = \mu_N g_N H_z I_z \pm \tfrac{1}{2}AI_z \pm \tfrac{1}{2}F(1 - 3\cos^2\theta)I_z \mp \tfrac{3}{2}F \times \sin\theta\cos\theta I_x + Q'_{zz}[I'^2_z - \tfrac{1}{3}I(I+1)] + Q'_{xxyy}(I'^2_x - I'^2_y) \quad (1)$$

which includes the nuclear Zeeman, the electron–nuclear contact hyperfine interaction, the pseudodipolar coupling whose magnitude is represented by F, and the nuclear quadrupole interaction, respectively. The plus and minus refer to the two electron spin states. The coefficients and operators of the quadrupole terms are primed because the quadrupole interactions are defined with respect to their own principal axis system (PAS). The complexity of the simulation and the number of unknown parameters is greatly reduced by ignoring the anisotropic components of the electron–nuclear dipolar interaction as in (1). Neglect of these terms may result in artifically narrow lines, and the relative peak intensities will not be correctly represented in the simulated spectrum, however, the transition frequencies will be correctly predicted by (1). The hyperfine contact coupling and principal values of the quadrupole interaction can therefore be accurately assigned by using this simplified Hamiltonian. It is these interactions that determine the number of lines and the line positions in the ESE

(16) Scott, R. A. Personal communication.
(17) Riester, J.; Kroneck, P. M. H.; Zumft, W. G. *Eur. J. Biochem.* **1989**, *178*, 751–762.
(18) McCracken, J.; Pember, S.; Benkovic, S.; Villafrance, J. J.; Miller, R. J.; Peisach, J. *J. Am. Chem. Soc.* **1988**, *110*, 1069–1074.
(19) Mims, W. B. *Phys. Rev.* **1972**, *B5*, 2409–2419.

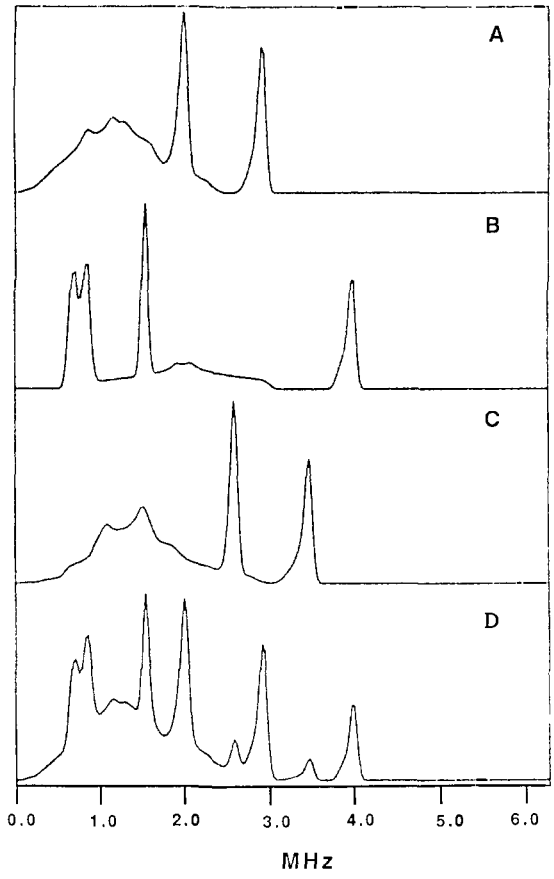

Figure 9. Simulated spin-echo envelope spectra for various nitrogenous ligands. The quadrupole coupling, e^2qQ/h (MHz), quadrupole asymmetry, η, and hyperfine contact couplings, A_{iso} (MHz), are (A) 1.44, 0.7, 0.6; (B) 1.53, 0.87, 1.65; (C) 2.3, 0.76, 0.65. Other conditions: $g = 2.03$, $B_0 = 3280$ G. The weighted intensities for spectrum D are 1.0 A, 0.8 B, and 0.2 C.

envelope spectrum. Furthermore, the extremely shallow modulation depth observed in the experimental results suggests that the anisotropic contribution to the hyperfine interaction is small so that neglecting the hyperfine anisotropy provides a good first-order approximation to the experimental frequency spectrum.

Spectra computed by using the Hamiltonian in (1) are the sum of the two nuclear quadrupole resonance spectra obtained for disordered solids computed for the effective Zeeman fields $(\omega_I \pm 1/2A)/\beta_n$. The resulting spectra are frequency histograms obtained by sampling orientations uniformly over the hemisphere. It is possible that a more accurate treatment of the orientational averaging process could be achieved by utilizing the angle selection scheme described by Hurst et al.[20] for simulating the ENDOR spectrum of randomly oriented transition-metal complexes. However, spherical averaging provides a better approximation at $g_\parallel$ than at other g values. Reasonable starting values for the quadrupole terms can be obtained from zero-field quadrupole frequency measurements.[21] Spectra were computed for the appropriate magnetic field value and for a range of quadrupole and hyperfine contact interactions.

The ESE envelope spectrum can be simulated by using three sets of ^{14}N quadrupole coupling parameters. The corresponding spectra are shown in Figure 9A–C. The computed spectrum shown in Figure 9A is obtained for an ^{14}N with $e^2qQ/h = 1.44 \pm 0.2$ Mhz, $\eta = 0.7 \pm 0.3$, and a hyperfine contact coupling, $A_{iso} = 0.6 \pm 0.1$ MHz. These quadrupole parameters are characteristic of a protonated distal nitrogen, N_1, but with an unusually small A_{iso}, on an imidazole ligand bound to Cu(II). The broad absorption centered at 1.2 MHz is comprised of the ν_0 and ν_- nitrogen quadrupole transitions in the upper and lower electron manifolds. This broad absorption is not observed in the experimental spectrum because of the finite spectrometer dead time (120 ns). Hyperfine anisotropy will further broaden these lines, making them even more difficult to detect experimentally. The two main narrow peaks at 1.9 and 2.9 MHz are the two $\Delta M_I = 2$ "double-quantum" nitrogen nuclear transitions, arising from the upper and lower electron mainfolds. When $A_{iso}/2 < \nu_N$, these "double-quantum" transitions are narrow compared to the single-quantum quadrupole transitions so that they are the only lines detected in the experimental spectrum. Unfortunately, the double-quantum lines are less sensitive to the quadrupole asymmetry, resulting in the relatively large uncertainty in η.

The spectrum computed for the second ^{14}N, shown in Figure 9B, is obtained for $e^2qQ/h = 1.53 \pm 0.2$ MHz, $\eta = 0.87 \pm 0.05$, and $A_{iso} = 1.65 \pm 0.05$ MHz. In model copper–imidazole complexes, hydrogen bonding of the N_1 nitrogen has been observed to increase e^2qQ/h by 0.1 MHz but has little effect on the quadrupole asymmetry.[22] The quadrupole parameters for the second nitrogen are therefore assigned to the distal nitrogen on an imidazole ligand bound to Cu(II). The hyperfine contact coupling of 1.65 MHz is closer to the value of 1.8–2.0 MHz typically observed for protonated imidazole ligands in type 1 and type 2 copper proteins and copper–imidazole complexes.[12] This value is close to the value that cancels the ^{14}N nuclear Zeeman splitting and gives rise to the narrow pure nuclear quadrupole resonance lines shown in Figure 9B.[13] The doublet centered at 0.8 MHz corresponds to the ν_0 and ν_- transitions while the narrow line at 1.5 MHz corresponds to the ν_+ transition in one of the electron manifolds. The line at 3.8 MHz corresponds to the $\Delta M_I = 2$ transition in the other electron manifold and occurs at approximately $2\nu_N + A_{iso}$. The broad absorption centered at 2 MHz arises from the ν_0 and ν_- transitions in this electron manifold. This broad absorption is not observed in the experimental spectrum because of the spectrometer dead time.

The spectrum computed for the third ^{14}N, shown in Figure 9C, is obtained for $e^2qQ/h = 2.3 \pm 0.2$ MHz, $\eta = 0.76 \pm 0.15$, and $A_{iso} = 0.65 \pm 0.1$ MHz. The comments made for the spectrum obtained for the first nitrogen, Figure 9A, apply equally well to the spectrum obtained from the third nitrogen. Only the double-quantum nitrogen quadrupole transitions in the two-electron manifolds are observed in the experimental spectrum. The quadrupole interaction of 2.3 MHz is close to that derived from NQR measurements on amide nitrogens[21] and also to that deduced from ESE measurements on substituted imidazole copper complexes.[22] However, for both the amide and the substituted imidazole nitrogens, the quadrupole asymmetry observed is much smaller than that derived from the present experimental results. But, as mentioned above, the double-quantum transitions are sufficiently insensitive to the value of the quadrupole asymmetry that either of these could be possible ligands.

The composite spectrum, shown in Figure 9D, is obtained by summing parts A–C of Figure 9. This spectrum reproduces the correct number of lines and the correct line positions of the experimental spectrum. As mentioned above, the broad absorption centered at 1.2 Mhz is not expected to be observed in the experimental spectrum because of the finite spectrometer dead time. Hyperfine anisotropy will further broaden the lines observed in the experimental spectrum compared to those computed by using (1).

Modulation from directly coordinated nitrogen ligands is not observed on the echo envelope in tetrahedral or square-planar copper complexes.[13] However, modulation from directly coordinated axial nitrogen ligands can be observed in five- or six-coordinate copper complexes.[23] In ESE studies of copper complexes with directly coordinated axial nitrogens, the quadrupole couplings were observed to be larger than those typically obtained for the distal nitrogen on imidazole ligands bound to Cu(II). It

(20) Hurst, G. C.; Henderson, T. A.; Kreilick, R. W. *J. Am. Chem. Soc.* **1985**, *107*, 7294–7299.
(21) Edmonds, D. T. *Phys. Rep.* **1977**, *29*, 233–290.
(22) Jiang, F.; McCracken, J.; Peisach, J. *XIII International Conference on Magnetic Resonance in Biological Systems*, **1988**; pp 17–19.
(23) Cornelius, J.; Peisach, J. Personal communication.

is therefore possible that the quadrupole interaction of 2.3 MHz could arise from an axially coordinated nitrogen on a five- or six-coordinate copper complex. This would most likely be on a copper in the mixed-valence half-met site since this possibility is consistent with the g values and Cu hyperfine splittings observed in the EPR spectrum.

Unusual EPR and ESE results have previously been reported for the Cu_A site in cytochrome c oxidase.[24] The EPR spectrum has poorly resolved copper nuclear hyperfine splittings and unusual g values.[24b] The spin-echo envelope modulation spectrum for the Cu_A also does not resemble the spectra typically observed for either type 1 or type 2 sites in copper proteins.[24c] An uncharacteristically shallow modulation depth was observed with modulation frequencies at 0.9, 1.5, 1.9, 3.2, and 4.3 MHz. The ESE results observed for cytochrome c oxidase, while highly anomalous compared to other copper proteins, are very similar to the results for N_2O reductase. In addition to the similarity in modulation depth, a matched set of lines for cytochrome c oxidase are observed in the ESE envelope spectrum of N_2O reductase. The lines at 0.9, 1.5, and 4.3 MHz in the spectrum of cytochrome c oxidase correspond to the lines at 0.8, 1.5, and 3.8 MHz in the spectrum of N_2O reductase. The double-quantum line at 4.3 MHz occurs at a slightly higher frequency because of a slightly larger hyperfine contact coupling compared to N_2O reductase.[25] The lines at 1.9 and 3.2 MHz observed for cytochrome c oxidase correspond to the lines at 1.9 and 2.9 MHz observed for N_2O reductase. The slightly larger frequency splitting between these lines in cytochrome c oxidase can again be accounted for by a slightly larger hyperfine contact coupling.[25] By analogy to the ESE envelope spectra for the Cu_A site in cytochrome c oxidase, we conclude that the two imidazole ligands assigned to the lines at 0.8, 1.5, 3.8 MHz and 1.9, 2.9 MHz in the spectrum of N_2O reductase are coordinated to the Cu_A site. This is consistent with the conclusion derived above that the nitrogenous ligand giving rise to the pair of lines at 2.5 and 3.4 MHz is coordinated to the half-met site.

The smaller hyperfine contact coupling observed for the two distal nitrogens on the imidazole ligands of the Cu_A site implies a reduced unpaired spin density on these N_1 nitrogens. This in turn suggests a reduced unpaired spin density on the directly coordinated (N_3) nitrogen of the imidazole ligand. Measurements of the hyperfine couplings for the N_3 nitrogens in N_2O reductase have not been reported as of this writing. However, in recent Q-band ENDOR studies on the Cu_A site in cytochrome c oxidase, Werst et al.[26] observed two ^{14}N ENDOR resonances corresponding to hyperfine contact couplings of 8.7 and 17.6 MHz, which are substantially smaller than the more typical values of 16–23 and 32–49 MHz for the two directly coordinated N_3 nitrogens in other copper proteins[27] and copper tetraimidazole model compounds.[28] Given the similarities between the ESE results on the Cu_A sites, we anticipate that the contact hyperfine couplings on the N_3 imidazole nitrogens in N_2O reductase will also be substantially reduced compared to type 1 and type 2 copper centers, analogous to the results for cytochrome c oxidase. We further expect that the N_1 and N_3 nitrogens with the smaller hyperfine contact couplings are part of the same imidazole ligand while those with the larger couplings belong to the second imidazole. The smaller hyperfine contact coupling on the N_3 nitrogen would also be expected to result in a reduced hyperfine anisotropy. Since the anisotropic components of the hyperfine interaction determines the depth of the modulation on the echo envelope wave form,[13,19] a reduced anisotropy is consistent with the unusually shallow modulation depth observed. However, we cannot exclude the possibility that other copper centers are present in the oxidized enzymes (such as those observed after dithionite reduction) which contribute to the echo intensity but do not contribute to the echo envelope modulation.

Finally, we note that our conclusions are consistent with those derived from resonance Raman,[10] EXAFS,[16] and magnetic circular dichroism (MCD)[29] data. Dooley et al. have reported a resonance Raman study of N_2O reductase and suggested that the activity correlates with the presence of a $Cu(II)S_2(cys)N(his)$ site.[10] EXAFS data suggest the presence of multiple copper sites with greater covalency than that usually observed for copper proteins.[16] Finally, both the EXAFS and MCD data on N_2O reductase appear to be remarkably similar to the data obtained for cytochrome c oxidase and different from those obtained for type 1 or type 2 copper proteins.

Conclusion

The spectroscopic model for the Cu sites in N_2O reductase that emerges from the present EPR and ESE study is that in the oxidized enzyme, between 70 and 85% of the copper ions are in the form of EPR-silent binuclear type 3 dimers. Between 15 and 30% of the copper ions are EPR active and are comprised of mixed-valent half-met sites and isolated cupric sites. The ESE data are also consistent with the presence of multiple chemically inequivalent Cu(II) sites with imidazole coordination. On the basis of the strong similarity of their ESE results, we conclude that the cupric sites are unusual Cu(II) sites, very similar to the Cu_A sites in cytochrome c oxidase. This is the first time that the Cu_A site has been observed in an enzyme other than cytochrome c oxidase. The additional frequencies in the ESE envelope spectra of N_2O reductase that are not observed in the spectra of cytochrome c oxidase most likely arise from an amide or substituted imidazole ligand coordinated to the EPR-active half-met site. Further evidence for the presence of a Cu_A site is obtained from the results of recent genetic sequencing studies on N_2O reductase[30] where the carboxy-terminal residues Cys-618 and -622, His-626, and Met-629 show a matched spacing and a conserved serin, resembling the proposed Cu_A site of cytochrome c oxidase subunit II.[31]

Deeper deuteron modulation is observed for the oxidized enzyme at pH 9.8, indicating that there are more deuterons associated with the EPR-active sites at higher pH. The ESE data indicate the presence of a coordinated deuterated ligand, most likely water or hydroxide. It is possible that this deuteron coupling is a consequence of either a pH-induced conformational change or a base-catalyzed proton exchange allowing enhanced access to the copper sites and accounting for the 10-fold increase in enzyme activity. It is more likely, however, that at pH 9.8 a new copper site becomes EPR active that has more exchangeable protons than the EPR-active copper sites present at pH 7.5.[32] This is consistent with the observed increase in the EPR susceptibility and broader line width for the enzyme at pH 9.8.

Acknowledgment. We gratefully acknowledge Sigrid Mümmler for isolation and biochemical characterization of the enzymes, Paul Tindall for constructing the slotted tube resonators, M. Bernardo for technical assistance with software for data collection, and W. B. Mims and E. I. Stiefel for stimulating discussions. We thank Dave Dooley and Bob Scott for communicating results prior to publication. We also thank a referee for many excellent suggestions on the manuscript. W.G.Z. was supported by the Deutsche Forschungsgemeinschaft and Fonds der chemischen Ind.

Registry No. Cu, 7440-50-8; N_2O reductase, 55576-44-8.

(24) (a) Beinert, H.; Griffiths, D. E.; Wharton, D. C.; Sands, R. H. *J. Biol. Chem.* **1962**, *237*, 2337–2346. (b) Stevens, T. H.; Martin, C. T.; Wang, H.; Brudvig, G. W.; Scholes, C. P.; Chan, S. I. *J. Biol. Chem.* **1982**, *257*, 12106–12113. (c) Mims, W. B.; Peisach, J.; Shaw, R. W.; Beinert, H. *J. Biol. Chem.* **1980**, *255*, 6843–6846.

(25) Thomann, H.; Bernardo, M.; George, G. N.; Prince, R., to be published.

(26) Werst, M.; Zimmerman, B.; Fee, J. A.; Hoffman, B. M., to be published.

(27) Roberts, J. E.; Cline, J. F.; Lum, V.; Freeman, H.; Gray, H. B.; Peisach, J.; Reinhammer, B.; Hoffman, B. M. *J. Am. Chem. Soc.* **1984**, *106*, 5324–5330.

(28) Van Camp, H. L.; Sands, R. H.; Fee, J. A. *J. Chem. Phys.* **1981**, *75*, 2098–2107.

(29) Dooley, D. M. Personal communication.

(30) Viebrock, A.; Zumft, W. G. *J. Bacteriol.* **1988**, *170*, 4658–4668.

(31) Holm, L.; Saraste, M.; Wilkstrom, M. *EMBO J.* **1987**, *6*, 2819–2823.

(32) We thank a referee for suggesting this possibility.